NEUROSURGERY

Magnetic Resonance Angiography of Giant Aneurysms. Pitfalls and Surgical Implications

ORLANDO DE JESUS MD; NATHAN RIFKINSON MD

Objective. **Magnetic resonance angiography (MRA) can be used to identify cerebral aneurysms. In this report, techniques for the diagnosis of giant cerebral aneurysm using MRA are discussed. Pitfalls in the diagnosis are presented.**

Background. **Giant cerebral aneurysms, which can be partially or totally thrombosed, or may have slow flow, can be confusing and difficult to diagnose. Giant cerebral aneurysms with thrombus formation, produce an artifact in time-of-flight MRA in which the thrombus simulates flowing blood.**

Method. **Five consecutive patients with the suspected diagnosis of giant cerebral aneurysm by MRA were analyzed. Neuroradiological studies were reviewed.**

Results. **In 20% of the cases, the correct diagnosis was made using MRA; in 60% of the cases, a correct diagnosis was made, but the size or the presence of flow was not correctly identified; in 20% of the cases, the diagnosis was incorrect. Four patients with giant cerebral aneurysms who presented a diagnostic and a therapeutic challenge are discussed.**

Conclusion. **Unless MRA findings are combined with computed tomography scan and magnetic resonance imaging findings, the exact nature of the sac contents of giant cerebral aneurysms cannot be identified.**

Keywords: Artifact giant cerebral aneurysm Magnetic resonance angiography Thrombus.

Magnetic resonance angiography (MRA), using a three-dimensional gradient-echo sequence, can be used to identify and delineate cerebral aneurysms by creating differences between flowing tissues and stationary tissues. Very fine angiograms are produced that can be totally rotated in space to visualize the circle of Willis. On some occasions, it is used to screen population at risk for aneurysms (1). Although MRA may delineate cerebral aneurysms, artifacts related to the technique may give a false impression of its size and contents. The purpose of this article is to present several cases of giant cerebral aneurysms diagnosed by MRA and to provide evidence for the necessity of combining several radiographic modalities for the correct characterization of giant cerebral aneurysms. Giant cerebral aneurysms are those with a diameter greater than 2.5 cm (2). They represent approximately 2.5% - 5% of all cerebral aneurysms. Most of these giant cerebral aneurysms impose diagnostic and therapeutic difficulties, since more than half are partially thrombosed. A completely thrombosed giant cerebral aneurysm is rare, reported in 1% to 16% of the cases (3), and is commonly associated with thrombosis of the parent artery (4). Giant cerebral aneurysms with slow flow or thrombus formation, may give an image different from the one obtained from the digital subtraction angiography (DSA). Vascular tumors may give an image similar to the one found in giant cerebral aneurysms.

Address correspondence to: Orlando De Jesús, MD, Section of Neurosurgery, Medical Sciences Campus, University of Puerto Rico, GPO Box 365067, San Juan, PR 00936 Tel. (787)765-8276.

Material and Methods

A review done at the University of Puerto Rico Medical Center over a 3-year period, between 1993 and 1995, identified ten patients with suspected diagnosis of a giant cerebral aneurysm at the initial diagnostic study. There were six females and four males. In five patients the diagnosis of giant cerebral aneurysm was confirmed by DSA without doing the MRA. In the remaining five patients, an MRA was done before the DSA. All MRA studies were initially analyzed by a neuroradiologist, the MRA findings were compared to the DSA findings, and

then correlated with the final pathology. These last five patients were used for our analysis and are discussed below.

Case 1. A 55 year-old male was transferred to our hospital with a rapid decrease in his level of consciousness. He entered another hospital due to a progressive, severe quadriparesis, respiratory dysfunction requiring a tracheotomy, and facial diplegia. Non-contrast head computed tomography (CT) scan showed a large round, calcified, midline posterior fossa lesion in the prepontine cistern, causing severe obstructive hydrocephalus (Fig. 1 upper left). He underwent a ventriculo-peritoneal shunt and gradually awakened and started to follow commands with eye-opening. He was scheduled for magnetic resonance imaging (MRI) and MRA. Due to his unstable blood pressure, only the MRA was performed, which revealed a large lesion related to the basilar artery trunk (Fig. 1 upper right). A DSA was done which did not show an aneurysmal sac or neck (Fig. 1 lower left), but an area of stasis of the dye along the posterior wall of the basilar artery in the venous phase (Fig. 1 lower right). We concluded that the lesion was an aneurysm that was completely thrombosed. Surgery was planned to decompress the brain stem. A left subtemporal presigmoid (petrosal) approach was used (5). After opening the dura, the aneurysm was identified, and proximal and distal controls were obtained. A fine needle was introduced into the hard, non-collapsible aneurysm sac and no blood was obtained. At this time it was confirmed that aneurysm was completely thrombosed so it was decided to trap and decompress the aneurysm in view of the presence of a good collateral supply. A permanent clip was placed on the basilar artery distal to the origin of the anterior inferior cerebellar arteries and another clip was placed proximal to the origin of the superior cerebellar arteries, no perforators were seen at the trapped segment. The aneurysm sac was opened and approximately two-thirds of its thrombus was removed. Post operatively the patient did well for except an ipsilateral third cranial nerve palsy.

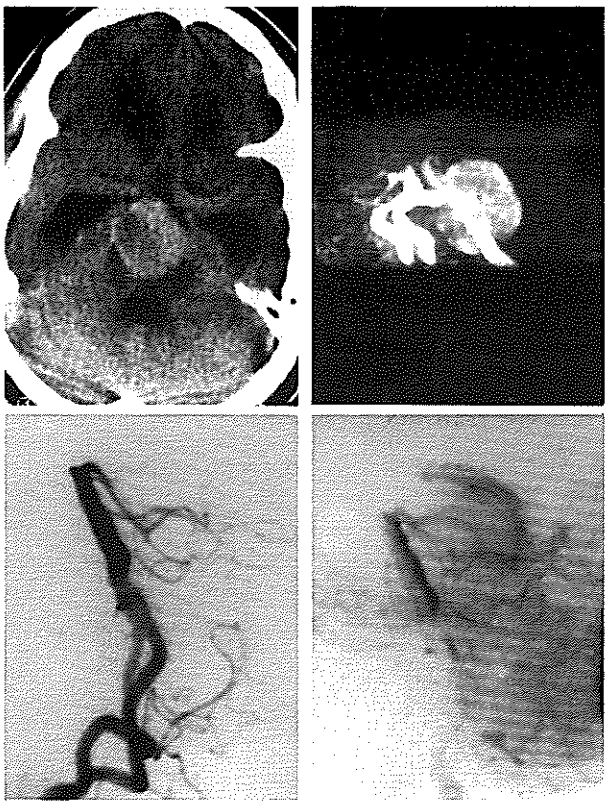

Figure 1. Upper left: Head CT scan without contrast showing a large hyperdense lesion occupying the prepontine cistern causing severe compression of the brain stem and obstructive hydrocephalus. Upper right: 3D time-of-flight MRA showing a 32 mm. spherical area of increased signal at the basilar artery trunk. Lower left: Lateral view of the DSA showing no aneurysmal sac or neck. Lower right: In the venous phase, there was an area of stasis of the dye along the posterior portion of the basilar trunk probably related to the irregularities caused by the thrombus located along the neck area.

Case 2. A 7 year-old male was admitted with a sudden complete left third cranial nerve palsy. This was associated with mild headache but no change in mental status. Non-contrast CT scan showed a 2.8 X 2.0 X 2.3 cm. hyperdense left parasellar lesion with densitometry similar to blood (Fig. 2 left). The sellar region appeared eroded. MRI showed a large sellar and suprasellar lesion with subacute blood at its posterosuperior margin (Fig. 2 center). MRA showed a lesion with two densities related to the left internal carotid artery and the parasellar area (Fig. 2 right). Since the subacute blood was associated with the supraclinoid artery, a DSA was done which showed an avascular lesion with no aneurysm formation. A prolactin level of 25,000 ng/ml, was reported and the patient was started on bromocriptine treatment.

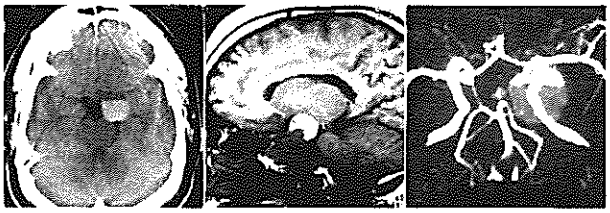

Figure 2. Left: Non-contrast head CT scan showing a left parasellar hyperdense lesion. Center: Non-enhanced T_1-weighted MRI, sagittal section, showing a sellar and suprasellar lesion with a hyperintensity at the superior pole of the lesion which probably represented a subacute clot. Right: MRA showing an increased signal intensity related to the left paraclinoid internal carotid artery.

Case 3. A 61 year-old female was admitted with a sudden complete right third cranial nerve palsy and numbness of the face along the V_1 and V_2 trigeminal distribution. CT scan showed a hyperdense parasellar mass. MRI revealed a 3 X 3.5 X 3.2 cm. mixed intensity lesion with a hyperintense peripheral rim (Fig. 3 left).

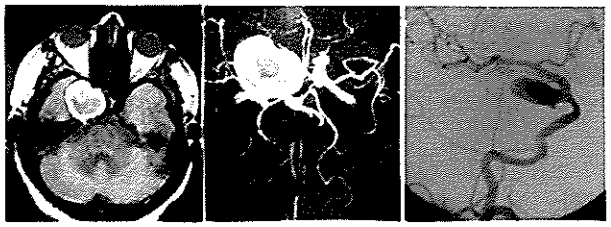

Figure 3. Left: MRI, axial section, showing a large right parasellar mixed intensity lesion, with a high intensity rim. Center: MRA showing a similar lesion at this location. Right: DSA revealed an aneurysm with a smaller patent lumen.

MRA showed a high signal intensity lesion at the same location with similar dimensions (Fig. 3 center). DSA showed filling of a cavernous aneurysm that was smaller than the MRI and MRA images (Fig. 3 right). At surgery, the aneurysm was found to be completely extradural. In view of the location and the age of the patient, a Selverstone clamp was placed on the common carotid and closed gradually to reduce the flow into the aneurysm.

Case 4. A 61 year-old female was admitted after a sudden, right-sided headache, nausea and blurred vision, followed by a brief loss of consciousness. Neurological examination showed nuchal rigidity without focal deficits. Head CT scan showed a hematoma in the right Sylvian fissure. The MRI revealed a 2 cm. mixed intensity lesion with peripheral edema also in the right Sylvian fissure (Fig. 4 left). MRA showed a lesion of similar diameter related to the bifurcation of the middle cerebral artery (MCA) with marked narrowing of the artery immediately preceding the lesion (Fig. 4 center). These findings suggested an aneurysm of the MCA with associated spasm. DSA showed what seemed to be a small aneurysm associated to the bifurcation of the MCA (Fig. 4 right). The patient was operated on the sixteenth day after her hemorrhage and a non thrombosed 7 mm. aneurysm was found after a large clot was removed from the Sylvian fissure.

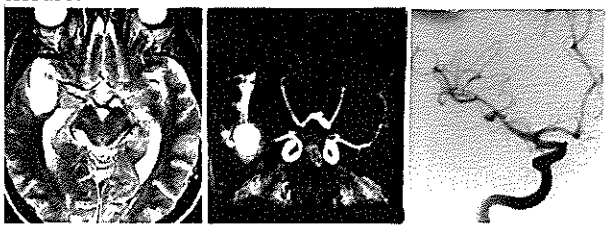

Figure 4. Left: T_2-weighted MRI, axial section, showing a 2 cm. mixed intensity lesion within the right Sylvian fissure. Center: MRA shows a 2 cm. increased signal intensity lesion at the MCA bifurcation with narrowing of the artery. Right: DSA revealed a 7 mm. aneurysm at the MCA bifurcation.

Results

In one patient, the diagnosis of giant cerebral aneurysm was correctly made using the MRA. The size suggested by the MRA was comparable with the size demonstrated by the DSA. In two patients the giant cerebral aneurysm was correctly identified by the MRA, but its size was incorrectly concluded. One patient had a partially thrombosed cavernous sinus aneurysm and the other had a small MCA aneurysm with an intracerebral clot surrounding the sac. In both cases, the size obtained from the MRA was larger than the true filling part of the aneurysm demonstrated by the DSA. One patient had a posterior fossa giant aneurysm in which the MRA showed flow inside the aneurysm, but the DSA showed no flow. It was confirmed at surgery that the aneurysm was completely thrombosed. In another patient, the diagnosis of a giant cerebral aneurysm was incorrectly made using the MRA. The image of the MRA suggesting a giant cerebral aneurysm was in fact that of a giant pituitary macroadenoma with hemorrhage. The intratumoral clot was confused with an aneurysmal sac. Table 1 summarizes

Table 1. Accuracy of MRA for size, flow, and diagnosis in patients with giant aneurysm

Case	Correct Size	Correct Flow	Correct Diagnosis
1	yes	no	yes
2	no	no	no
3	no	yes	yes
4	no	yes	yes
5	yes	yes	yes

the findings for each patient. In 20% of the cases, the correct and exact diagnosis was made using MRA; in 60% a correct diagnosis was made but the size, or the presence of flow, was not correctly identified; in 20% the diagnosis was incorrect.

Discussion

MRA is a truly non invasive and useful method to examine cerebral aneurysms, but artifacts can be produced due to the techniques used to characterize the aneurysms. This is frequently seen in giant aneurysms since partial thrombosis occurs in 48-76% of the cases (6). The high incidence of thrombus formation within a giant cerebral aneurysm is related to the critical ratio between the aneurysmal volume and the aneurysmal neck size (7). Unless a giant cerebral aneurysm is completely thrombosed, there is no protection against subarachnoid hemorrhage. In those cases in which the aneurysm is completely thrombosed, surgery is done to decompress the neural structures. When operating a tumor, the diagnostic possibility of a giant thrombosed aneurysm has to be kept in mind, even if angiography has been performed. In the four cases presented, the combination

of MRA, CT, and MRI findings helped us to correctly identify and characterize the aneurysms. These findings facilitate the organization of specific management strategies for each case.

Partially thrombosed giant aneurysms produce a flow void in the MRI and different signal intensities from the various stages of the clot (8). There are certain limitations in the use of MRA with giant aneurysms. Slow flow and turbulent flow lesions are poorly visualized owing to the saturation of the moving spins residing for too long within the excited volume, so MRA will underestimate the size of larger aneurysms (9,10). Subacute, intraluminal thrombus produces an artifact which falsely simulates flowing blood on the maximum intensity projection (MIP) (9,11). Edelman et al. reported that MRA fails to detect thrombosed cerebral aneurysms and those containing very slow flow (9). Schuirer et al. recognized that partially or completely thrombosed cerebral aneurysms can appear as a vascular structure on MRA, and that dolichoectatic vessels, or large aneurysms with slow flow, may have a loss of signal due to the saturation effect, so that they cannot be detected by the MIP algorithm (12).

Time-of-flight (TOF) imaging relies primarily on flow related enhancement produced by flowing blood which yields a greater signal intensity than the surrounding stationary tissue. Non saturated spins, like blood, moving into the image, will appear as a high signal when compared to saturated spins from stationary tissues. A major limitation of the TOF is its relative inability to cancel signal from stationary spins. In particular, short T_1 material, such as fatty tissues and subacute hematoma containing methemoglobin, will appear bright, simulating flow enhancement. The MIP algorithm cannot discriminate between flow-related enhancement and subacute thrombus; as a result, both are simultaneously projected as hyperintensity. Lewis et al. found that the signal loss from progressive saturation of inflowing spins can be partially controlled by using thinner imaging volumes or 2-D images (13). However, TOF MRA has the advantage of using a shorter TE, thus it is less susceptible to signal loss.

Phase-contrast (PC) imaging relies primarily on velocity induced phase shifts to distinguish flowing blood from stationary tissues. Two or more acquisitions with opposite polarity of the bipolar flow-encoding gradients are subtracted to produce an image of the vascularity. Because stationary tissues yield no phase shifts, a substraction of the acquisition results in cancellation of the stationary tissue signal. The background is completely suppressed, so bright fat and thrombus are suppressed. The PC MRA shows only the patent lumen of the aneurysm in a manner analogous to conventional angiogram (14). Blood flow in an aneurysm is remarkably complex and changes during the cardiac cycle (15). In addition, the flow velocity in the aneurysm is much slower than in the parent artery. Therefore, these complex, slow and disturbed flows are the major mechanisms of loss of signal on the 3-D PC technique. Non laminated turbulent flow may cause a significant loss of signal on the PC MRA.

Houston et al. found that cerebral aneurysms smaller than 15 mm were equally demonstrated in the TOF and the PC imaging techniques, but in larger aneurysms the PC technique was superior (14). The use of gadolinium enhancement improves the visualization of the vasculature, but also increases the background noise with TOF imaging due to enhancement of normal structures, such as the nasal mucosa, choroid plexus, and pituitary gland (14). Table 2 lists the advantages and disadvantages of both techniques. Although Houston reported that MRA had a sensitivity of 75% - 87.5% to detect cerebral aneurysms greater than or equal to 5 mm, they had a case in which a thrombus was incorrectly identified as a large aneurysm (16).

Tsuruda had used a direct comparison of the MRA with the T_1-weighted spin-echo images to distinguish between thrombus and flow-related enhancement in cerebral aneurysms treated by endovascular balloon occlusion (17). Thrombus has a similar appearance on both studies, whereas flow-related enhancement on MRA should be replaced by flow void on the spin-echo study. A giant cerebral aneurysm filled with subacute thrombus with shortened T_1 may cause a high signal intensity on a 3-D TOF MRA and no signal on 3-D PC MRA. However, DSA or conventional angiography will definitely confirm if there is blood flow within the aneurysm. Due to the frequent presence of clots within these aneurysms, angiograms will often underestimate the true size of the aneurysm. Despite MRA advantages over DSA, the characterization of giant cerebral aneurysms by MRA will depend on its

Table 2. Advantages and disadvantages of MRI pulse sequences

	Time of flight	Phase contrast
Advantages	1. Shorter time to perform 2. Minimal signal loss arising from pulsatile and complex flows	1. Fat and thrombus are suppressed 2. Potential for qualitative flow measurements 3. Better definition of smaller vessels
Disadvantages	1. Inability to distinguish flow from thrombus 2. Use of gadolinium increases the background noise	1. Longer time to perform 2. Slow flow produces loss of signal

combination with other techniques. MRA functions primarily as a screening tool and should always be interpreted with other imaging modalities (18).

Conclusions

The cases presented illustrate the idea that although giant cerebral aneurysms can be detected by MRA, a problem arises in the characterization for flow and size. The easiest way to identify and characterize an aneurysm is by doing a DSA, but if the data obtained from the MRA is combined with that of the CT scan and the MRI, a clear picture can most of the times be obtained using these non invasive studies. The use of this principle is helpful in avoiding complications in diagnosis and management.

Resumen

La angiografía por resonancia magnética se está utilizando para detectar aneurismas cerebrales. El diagnóstico de aneurismas cerebrales gigantes puede ser confuso y difícil de obtener. En este estudio se analizaron cinco pacientes consecutivos con el diagnóstico presuntivo de aneurisma cerebral gigante. En 20% de los casos se obtuvo un diagnóstico correcto y en 20% de los casos se obtuvo un diagnóstico incorrecto. En los restantes casos se obtuvo un diagnóstico correcto pero se identificó incorrectamente el tamaño del aneurisma o la presencia de flujo arterial. Se recomienda que se combinen los hallazgos de la angiografía magnética con los de la tomografía computarizada y la imagen de resonancia magnética para la identificación de los aneurismas cerebrales gigantes.

References

1. Spritzer CE, Pelc NJ, Lee JN, Evans AJ, Sostman HD, Riederer SJ. Rapid MR imaging of blood flow with a phase-sensitive, limited-flip-angle, gradient recalled pulse sequence: preliminary experience. Radiology 1990;176:255-262.
2. Morley TP, Barr HWK. Giant intracranial aneurysm: diagnosis, course, and management. Clin Neurosurg 1969;16:73-94.
3. Gerber S, Dormont D, Sahel M, Grob R, Foncin JF, Marsault C. Complete spontaneous thrombosis of a giant intracranial aneurysm. Neuroradiology 1994;36:316-317.
4. Keravel Y, Sindou M. Mechanism of formation: pathological features. In: Keravel Y, Sindou M, Pialat J, Szapiro J, Garcia-Orjuela C, Tommasi M, eds. Giant intracranial aneurysms: therapeutic approaches. Berlin, Spring-Verlag, 1988; 4-11.
5. Al-Mefty O, Fox JL, Smith RR. Petrosal approach for petroclival meningiomas. Neurosurg 1988;22:510-517.
6. Rosta L, Battaglia R, Pasqualin A, Beltramello A. Italian cooperative study on giant intracranial aneurysm: radiological data. Acta Neurochir 1988;42(Suppl):53-59.
7. Whittle IR, Dorsch NW, Besser M. Spontaneous thrombosis in a giant intracranial aneurysm. J Neurol Neurosurg Psychiatry 1982;45:1040-1047.
8. Grossman RI, Yousem DM. Techniques in Neuroimaging. In: Thrall JH, ed. Neuroradiology. The requisites. St. Louis, Mosby, 1994; 1-23.
9. Edelman RR, Mattle HP, Atkinson DJ, Hoogewoud HM. MR angiography. AJR 1990;154:937-946.
10. Ross IS, Masaryk TJ, Modic MT, Ruggieri PM, Haacke EM, Selman WR. Intracranial aneurysms: evaluation by MR angiography. AJNR 1990;11:449-456.
11. Sevick RJ, Tsuruda JS, Schmalbrock P. Three-dimensional time-of-flight MR angiography in the evaluation of cerebral aneurysm. J Comp Assist Tomogr 1990;14:874-881.
12. Schuirer G, Huk WJ, Laub G. Magnetic resonance angiography of intracranial aneurysms: comparison with intra-arterial digital substraction angiography. Neuroradiology 1992;35:50-54.
13. Lewis JS, Laub G. Intracranial MR angiography: a direct comparison of three time-of-flight techniques. AJNR 1991;12:1133-1139.
14. Huston J III, Rufenacht DA, Ehman RL, Wieben DO. Intracranial aneurysms and vascular malformations: comparison of time-of-flight and phase-contrast MR angiography. Radiology 1991;181:721-730.
15. Araki Y, Kohmura E, Tsukaguchi I. A pitfall in detection of intracranial unruptured aneurysms on three-dimensional phase-contrast MR angiography. AJNR 1994;15:1618-1623.
16. Houston J III, Nichols DA, Luetmer PH, Goodwin JT, Meyer FB, Wiebers DO, Weaver AL. Blinded prospective evaluation of sensitivity of MR angiography to known intracranial aneurysms: importance of aneurysm size. AJNR 1994;15:1607-1614.
17. Tsuruda JS, Servick RJ, Halbach VV. Three-dimensional time-of-flight MR angiography in the evaluation of intracranial aneurysms treated by endovascular balloon occlusion. AJNR 1992;13:1129-1136.
18. Gewirtz RJ, Awad IA. Giant aneurysm of the proximal anterior cerebral artery: report of three cases. Neurosurgery 1993;33:120-125.